ELSEVIER

PII: S0955-7997(97)00044-1

Engineering Analysis with Boundary Elements **20** (1997) 45–49

0955-7997/97/$17.00

Wave height distributions around submerged structure in wave–current field

Chung-Ren Chou, Shinn-Shan Yan & Hui-Ming Fang

Department of Harbor and River Engineering, Taiwan Ocean University, Pei-Ning Rd. 2, Keelung 202, Taiwan

Effects of submerged structure on a wave–current field are studied numerically by means of BEM. The potential flow field is assumed to be composed of a steady current potential and an unsteady wave potential, where the Doppler effect is taken into consideration. The current velocities affected by the submerged structures were determined by using the three-dimensional boundary element method. Dispersion relations affected by the presence of current are used to calculate the apparent wave frequencies. Wave height distributions in the wave–current field were estimated. © 1997 Elsevier Science Ltd.

Key words: BEM, Doppler effect, wave height distributions.

1 INTRODUCTION

Intensive studies on wave–current interactions have been carried out by many researchers theoretically or numerically. The concept of radiation stress was first introduced by Longuet-Higgins and Stewart[1]. Ship motions in wave–current field were studied by Newman[2]. Wave diffraction and deflections by submerged structures in a uniform current field were discussed by Grue and Palm[3]. Matsui et al.[4] analyzed forces on a vertical cylinder in a wave–current field through perturbation analysis by using potential flow theory.

Studies on wave–current interactions have usually been based upon the assumption that wavelengths will be affected while their frequencies remain unchanged (see, e.g. Longuet-Higgins and Stewart[1]). The assumption can be questioned, since the Doppler effect states that the angular frequency will be affected by current velocity. In this paper, both current and wave are assumed to be small, therefore the velocity potential in the wave–current field can be treated as a composition of a steady current velocity potential and an unsteady wave potential. The same assumption was also used by Newman[2].

First, in this paper, the velocity field around the submerged structure due to the current is calculated by means of the three-dimensional boundary element method. The apparent wave frequency affected by the current can be calculated, which means the Doppler effect is taken into consideration. Second, the three-dimensional boundary element method is used again to calculate the velocity potential around the submerged structure that is induced by wave, while the apparent wave frequency should be used for the boundary condition on the water surface. Finally, the total velocity potential in the wave–current field can be obtained by the superposition of the velocity potential induced by current and wave. The distributions of wave height around the submerged structure are shown.

2 THEORETICAL ANALYSIS AND NUMERICAL SCHEME

Figs 1 and 2 show the definition sketches for the cases to be studied, where the submerged structures are located on the sea floor. The Cartesian coordinate system (x,y,z) is adopted and the x–y plane is located on the water surface with the z-axis positively upwards. A pseudo-boundary is located far away from the submerged structure; previous works done by Chou and Han[5] have shown that approximately half of an incident wave length will be enough. The fluid field is divided into two parts by the pseudo-boundary, where region I is an open sea region with constant depth h and region II is a closed domain with uneven sea floor. The fluid is assumed to be invicid, incompressible and the flow is irrotational, the flow in both regions will have velocity potential Φ that satisfies the following Laplace equation.

$$\frac{\partial^2\Phi}{\partial x^2}+\frac{\partial^2\Phi}{\partial y^2}+\frac{\partial^2\Phi}{\partial z^2}=0 \quad (1)$$

As shown in Figs 1 and 2, current with velocity U_0 comes

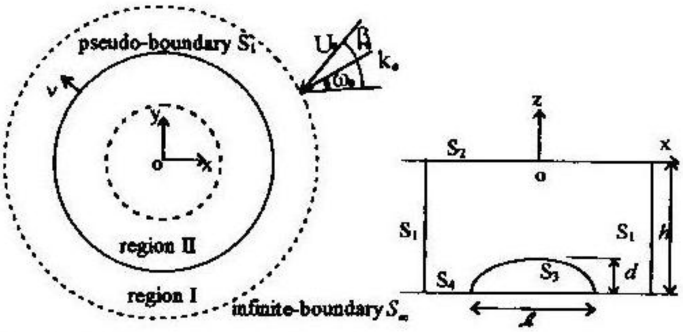

Fig. 1. Definition sketch of a submerged structure with semi-spherical shape.

from infinity intersects the x-axis with an angle β_0 together with a small amplitude wave with angular frequency σ_0 ($= 2\pi/T$, where T is the wave period), amplitude ζ_0 incidence from infinity intersects the x-axis with an angle ω_0. The velocity potential Φ is composed of two parts: the velocity potential Φ^c induced by the steady current, and the velocity potential Φ^w induced by the unsteady wave under consideration of the Doppler effect as follows:

$$\Phi = \Phi^c + \Phi^w \tag{2}$$

where both Φ^c and Φ^w satisfy the Laplace equation.

2.1 Velocity potential of steady current

The potential function of the uniform current region I is a result of undisturbed potential φ^0 of the current velocity with velocity U_0 incident from the open sea, and the disturbed potential φ^* that is induced by the presence of the submerged structure:

$$\varphi^{(1)} = \varphi^0 + \varphi^* \tag{3}$$

where $\varphi^0 = -U_0(x\cos\beta_0 + y\sin\beta_0)$. It is noted that away from the submerged structure, the disturbed potential of current, φ^*, can be neglected.

Region II is a closed three-dimensional domain which is bounded by the pseudo-boundary S_1, the water surface S_2, the submerged structure fixed on sea floor S_3 and the impermeable uneven sea bed S_4. According to Green's second identity, the potential $\varphi^{(2)}$ in region II can be determined by the following integral equation,

$$c\varphi^{(2)}(x,y,z) = \frac{1}{4\pi}\int_s \left[\bar{\varphi}^2(\xi,\eta,\zeta)\frac{1}{R} - \varphi^{(2)}(\xi,\eta,\zeta)\frac{\partial}{\partial \nu}\frac{1}{R}\right] \mathrm{d}S \tag{4}$$

where $\varphi^{(2)}(\xi,\eta,\zeta)$ and $\bar{\varphi}^{(2)}$ (ξ,η,ζ)($= \partial\varphi^{(2)}/\partial\nu$) are the potential and its normal derivative with ν local normal vector to boundary taken outwards, $S = S_1 + S_2 + S_3 + S_4$, and $R = [(x-\xi)^2 + (y-\eta)^2 + (z-\zeta)^2]^{1/2}$ is the distance between an inner point (z,y,z) and the point (ξ,η,ζ) on boundary S. The factor c is equal to unity within boundary, but will be 1/2 on a smooth boundaries.

In the numerical analysis, the boundary S, where $c = 1/2$ is discretized into N constant plane elements, eqn (5) can be written in a matrix form as,

$$\{\varphi^{(2)}\} = \{k\}\{\bar{\varphi}^{(2)}\} \tag{5}$$

where $\{\varphi^{(2)}\}$ and $\{\bar{\varphi}^{(2)}\}$ are the potential function and its normal derivative on the boundary S, respectively. $\{k\}$ is a coefficient matrix related to the geometric shape of the boundary. The numerical scheme is discussed in detail by Chou and Han [5].

The boundary conditions for the cases under consideration are summarized as follow:

1. Free surface condition: assuming that the variations of the water level due to the current can be neglected.

$$\bar{\varphi}^{(2)} = 0, \quad z = 0 \tag{6}$$

2. Boundary condition on the impermeable sea bed and the submerged structure. The flow is nil in the normal direction on an impermeable surface.

$$\bar{\varphi}^{(2)} = 0 \tag{7}$$

3. Boundary condition on the pseudo-boundary S_1: according to the continuity of mass and energy fluxes between region I and region II on the pseudo-boundary S_1, we have the following relationship.

$$\bar{\varphi}^{(2)} = \bar{\varphi}^{(1)} \tag{8}$$

$$\varphi^{(2)} = \varphi^{(1)} \tag{9}$$

To facilitate substitution of the boundary conditions, eqn (5) is first decomposed into four sub-matrices containing contributions from the pseudo-boundary S_1, the free surface S_2, the boundary of the submerged structure S_3, and the boundary at the sea floor S_4, respectively. These boundaries are divided into N_1, N_2, N_3 and N_4 constant plane elements, with the total number of elements equal to N ($= N_1 + N_2 + N_3 + N_4$), eqn (5) can be expressed as

$$\{\varphi^{(2)}_{ij}\} = \{k_{ij}\}\{\bar{\varphi}^{(2)}_{ij}\} \quad (i,j = 1\text{–}4) \tag{10}$$

Together with eqn (2) and the boundary conditions from eqns (6)–(9), potential functions on the boundaries can be calculated.

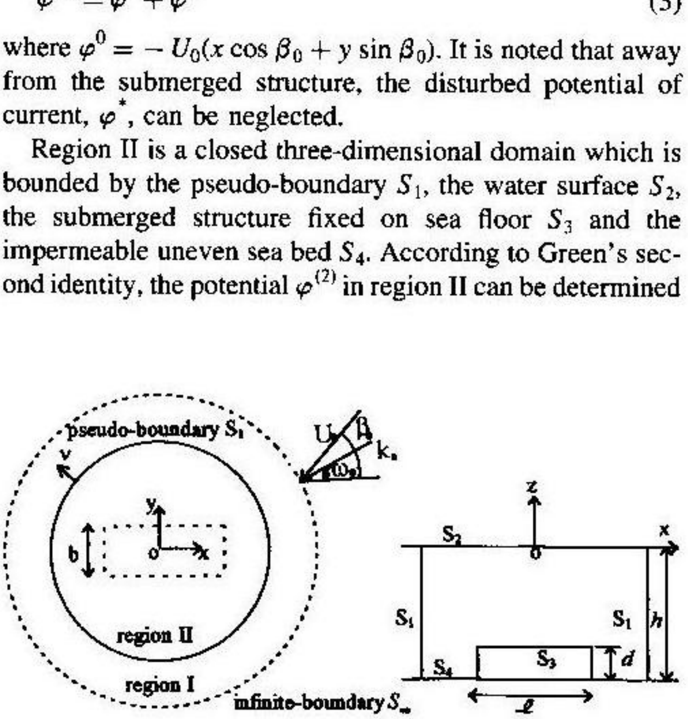

Fig. 2. Definition sketch of a submerged structure with rectangular cross-section.

2.2 Unsteady wave velocity potential

The wave is assumed to incidence from the open sea region far away from the boundary, with an angular frequency σ_0, an amplitude ζ_0, and a wave number k_0. The wave intersects the positive x-axis with an angle ω_0. Assuming the Froude number based upon the current velocity as well as the wave amplitude are small, the potential function for waves can be expressed as,

$$\Phi^W(x,y,z;t) = \frac{g\zeta_0}{\sigma_0}\phi(x,y,z)e^{-i\sigma t} \tag{11}$$

where $i=\sqrt{-1}$ is the imaginary constant, t is the time, ϕ is the dimensionless potential function satisfying the Laplace equation, and σ is the apparent frequency due to current.

$$\sigma = \sigma_0 + \vec{k}\cdot\vec{U} \tag{12}$$

with $|\vec{k}| = k_0$, $|\vec{U}|$ is the current velocity for any point within the region.

The wave potential function in region I, $\phi^{(1)}$, is a combination of the potential function of the incident wave, ϕ^0, and the diffracted wave potential due to the structure on the sea floor, ϕ^*.

$$\phi^{(1)}(x,y,z) = \phi^0(x,y,z) + \phi^*(x,y,z) \tag{13}$$

Since it is assumed that the pseudo-boundary with constant depth, by separating the variables, potential function $\phi^{(1)}$ in region I can be expressed as,

$$\phi^{(1)}(x,y,z) = \left[f^0(x,y) + f^*(x,y)\right]\frac{\cosh\left[k_0(z+h)\right]}{\cosh(k_0h)} \tag{14}$$

By substituting eqn (14) into the Laplace equation, we obtained the potential function f^* which satisfies the following Helmholtz equation,

$$\frac{\partial^2 f^*}{\partial x^2} + \frac{\partial^2 f^*}{\partial y^2} + k_0^2 f^* = 0 \tag{15}$$

At the far field S_∞, f^* must satisfy the Sommerfeld radiation condition. According to Green's second identity, the velocity potential in region I can be obtained from the following integral equation on the boundary,

$$cf^*(x,y) = \frac{i}{4}\int_{\Gamma_1}\left\{\bar{f}^*(\xi,\eta)H_0^{(1)}(k_0r) - f^*(\xi,\eta)\frac{\partial}{\partial \nu} \times \left[H_0^{(1)}(k_0r)\right]\right\}ds \tag{16}$$

where $f^*(\xi,\eta)$ is the potential function on the boundary, $\bar{f}^*(\xi,\eta)(=\partial f^*/\partial\nu)$ is its normal derivative with ν local normal coordinate to the boundary taken outwards, Γ_1, is the pseudo-boundary, and $H_0^{(1)}$ is the zeroth-order Hankel function of the first kind. As stated before, the coefficient c equals 1 within the boundaries, but will have a value of 1/2 on a smooth boundary. In this case, the boundary S_1 was divided into M constant line elements, therefore eqn (16) is discretized and written in a matrix form as

$$\{F^*\} = \{K^*\}\{\bar{F}^*\} \tag{17}$$

where $\{F^*\}$ and $\{\bar{F}^*\}$ are the potential function and its normal derivative on the pseudo-boundary Γ_1, respectively. $\{K^*\}$ is a coefficient matrix, and is determined by the geometric shape of the boundary.

The wave potential function in region II, $\phi^{(2)}$, as stated in Section 2.1, can then be expressed as

$$\{\phi_{ij}^{(2)}\} = \{K_{ij}\}\{\bar{\phi}_{ij}^{(2)}\ (i,j=1\text{–}4) \tag{18}$$

The boundary conditions of which are summarized as follow:

1. The water surface boundary condition: assuming both current speed and wave motion are small, the free water surface boundary condition for waves subjected to the Doppler effect is expressed as[2],

$$\frac{\partial\phi^{(2)}}{\partial z} = \frac{\sigma^2}{g}\phi^{(2)},\quad z=0 \tag{19}$$

where σ can be calculated from eqn (12).

2. Boundary condition on the impermeable sea bed and submerged structure: since the surfaces are impermeable, the flow is nil in the normal direction, i.e.

$$\bar{\phi}^{(2)} = 0 \tag{20}$$

3. Boundary condition on the pseudo-boundary S_1: requirement of continuity for mass and energy fluxes between region I and region II at the pseudo-boundary S_1 leads to the following expressions.

$$\bar{\phi}^{(2)} = \bar{\phi}^{(1)} \tag{21}$$

$$\phi^{(2)} = \phi^{(1)} \tag{22}$$

The pseudo-boundary S_1 is divided into N elements in the z-direction, and M elements in the horizontal direction, with the boundary conditions shown in eqns (14), (21) and (22), the potential function, $\phi_1^{(2)}$, and its normal derivative, $\bar{\phi}_1^{(2)}$, on the pseudo-boundary are related as

$$\{\phi_1^{(2)}\} = \{R\}\{F^0 - K^*\bar{F}^0\} + C\{R\}\{K^*\}\{Q\}\{\bar{\phi}_1^{(2)}\} \tag{23}$$

where $C = k_0/N_0\sinh(k_0h)$, with $N_0 = 1/2 + k_0h/\sinh(2k_0h)$. The coefficient matrices $\{R\}$ and $\{Q\}$ have been discussed in detail by Chou and Han[5]. By substituting eqns (19), (20) and (23) into eqn (18), we obtained

$$\begin{Bmatrix} [K_{11} - CRK^*Q] & \frac{\sigma^2}{g}K_{12} & 0 \\ K_{21} & \frac{\sigma^2}{g}K_{22} - I & 0 \\ K_{31} & \frac{\sigma^2}{g}K_{32} & -I \end{Bmatrix}\begin{Bmatrix}\bar{\phi}_1^{(2)} \\ \bar{\phi}_2^{(2)} \\ \bar{\phi}_3^{(2)}\end{Bmatrix} = \begin{Bmatrix} R[F^0 - K^*\bar{F}^0] \\ 0 \\ 0 \end{Bmatrix} \tag{24}$$

The pressure at any point within the wave–current field can be calculated by using the Bernoulli equation; moreover, the air pressure on the free surface is assumed to be constant and thus can be neglected, therefore, the surface elevations in region II can be expressed by:

$$\zeta = -\frac{1}{g}\left[\frac{\partial \Phi^W}{\partial t} + \nabla\Phi^C \cdot \nabla\Phi^W\right] \tag{25}$$

Applying eqn (11), the ration between the surface elevation, ζ, and the amplitude of the incident wave, ζ_0, can be expressed as $K_d(=\zeta/\zeta_0)$ through:

$$K_d = \frac{1}{\sigma_0}|i\sigma\phi^{(2)} - \nabla\varphi^{(2)} \cdot \nabla\phi^{(2)}| \tag{26}$$

3 RESULTS AND DISCUSSIONS

Two examples are presented and discussed in this paper, including a submerged structure having a semi-spherical shape with a diameter l; and a rectangle section with dimension $l \times b \times d$ (length × width × height).

As stated above, the Froude number F_r can be expressed by the current velocity U_0 and the water depth h. Throughout the calculation, the Froude number is taken as $F_r = 0.1$, the incident angle of the waves is set to be $\omega_0 = 0°$, and the wave number, $k_0h = 1.0$ ($\sigma_0^2 h/g = 0.762$) is used. During the calculation, angles between waves and current, $\theta_0(=\beta_0 - \omega_0)$, were varied. Five different values for the intersection angle $\theta_0 = 0°$, 45°, 90°, and 180° were used to demonstrate the effects of the wave–current interactions.

3.1 A semi-spherical structure

As shown in Fig. 3, the wave height distributions are for the cases with the reservation that the dimensionless wave numbers $k_0h = 1.0$. Fig. 3a is a case without current, it shows that waves behind the submerged structure are larger than those in the front, the reason may be the diffraction due to the structure. Fig. 3b shows that when waves

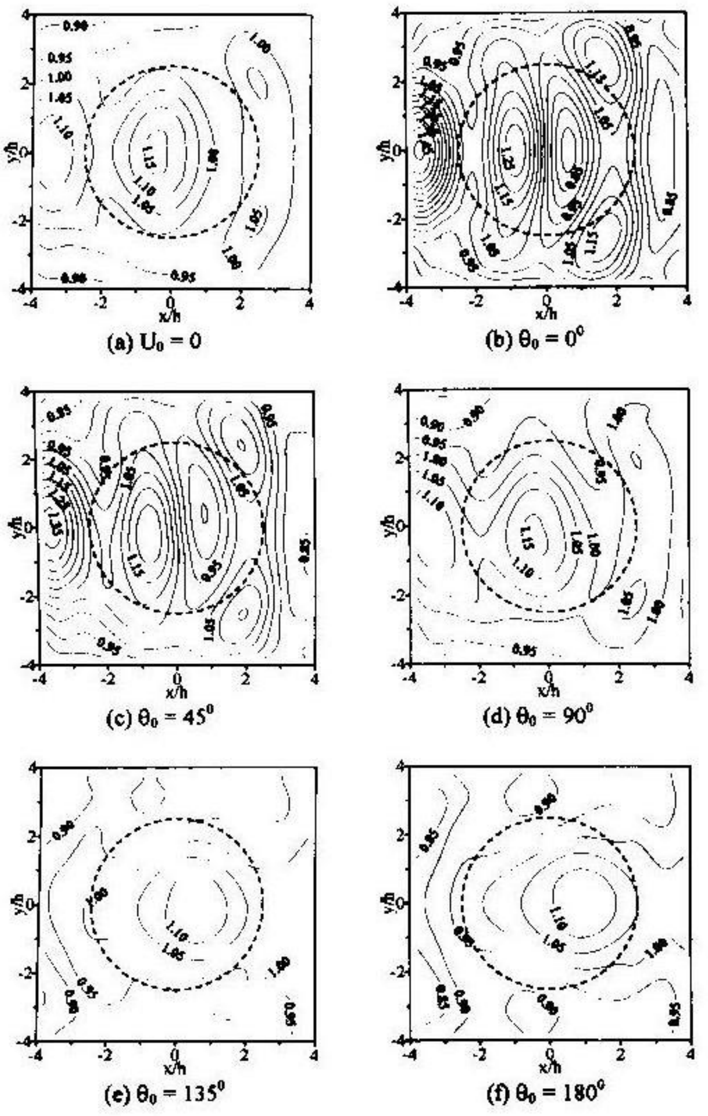

Fig. 3. Wave height distributions in region II for a spherical shaped structure. $k_0h = 1.0$, $\omega_0 = 0°$, $F_r = 0.1$.

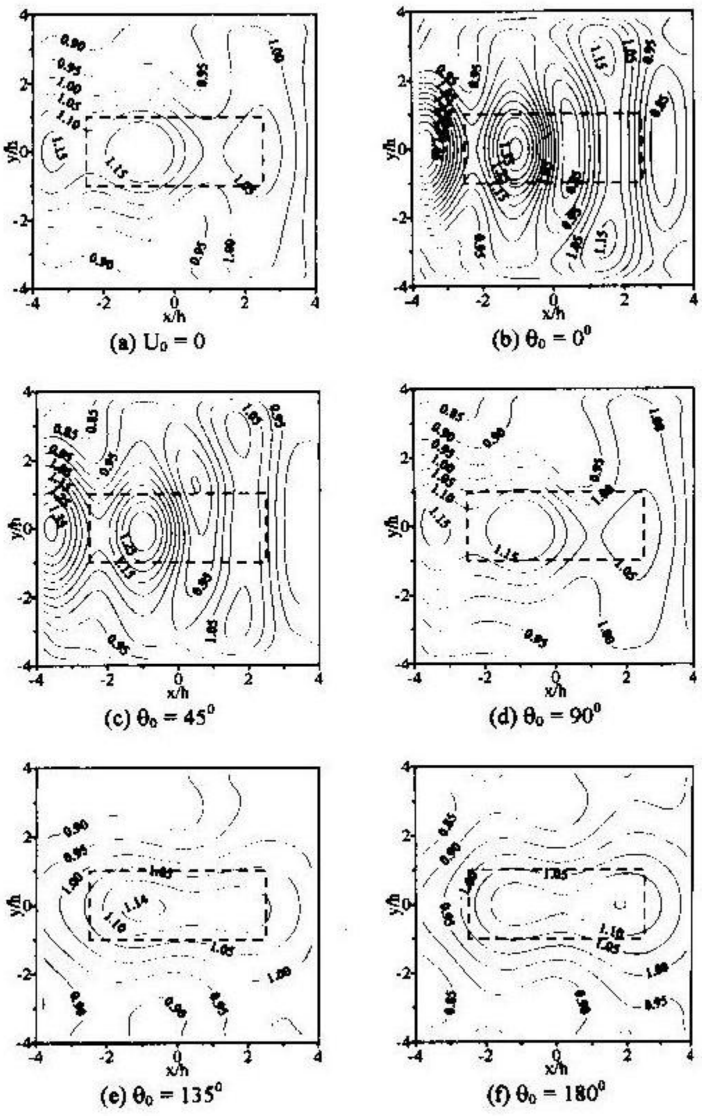

Fig. 4. Wave height distributions in region II for a rectangular section. $k_0h = 1.0$, $\omega_0 = 0°$, $F_r = 0.1$.

travel on the same direction as the current, i.e. $\theta_0 = 0°$, wave heights increase because the diffraction behind the structure is exaggerated due to the Doppler effect; therefore the distribution of wave height is symmetrical along the direction of incidence wave, i.e. the x-axis. With an intersection angle $\theta_0 = 45°$ shown in Fig. 3c, wave heights are larger than those of cases without current; however, since the flow velocities are not symmetrical about the direction of incident wave, wave heights are unevenly distributed and are shifted toward the negative y-direction. With $\theta_0 = 90°$ shown in Fig. 3d, the wave heights distribution seems to be similar to the case without current, but with some residual component current velocities aroused by the submerged structure. These marginal effects on wave height distributions are discernible by the asymmetrical wave height distributions about the direction of incident wave. Finally, for the cases with $\theta_0 = 135°$ and 180° as shown in Fig. 3e and Fig. 3f, respectively, with the result that the wave interacted with adverse current in the x-direction, the wave heights decreased due to the reduction of apparent angular frequencies.

3.2 A rectangular cylindrical structure

The boundaries are divided into a total number of 2024 constant plane elements, where the respective element numbers for each boundary are: $N_1 = 512, N_2 = 1024, N_3 = 272, N_4 = 216$.

Fig. 4 shows cases with a dimensionless wave number $k_0h = 1.0$. Fig. 4a shows a case without current, the wave height distribution seems to be similar as the previous case shown in Fig. 3a. Furthermore, from the cases shown in Fig. 4b–f, the angle between waves and current increases from $\theta_0 = 0°$ to 180°, and the wave height distribution also appears similar to results shown in the previous case, i.e. Fig. 3b–f, under similar conditions.

4 CONCLUSION

First of all in this paper the three-dimensional boundary element method is applied to obtain the distribution of current field. Second, the Doppler effect is used to express the dispersion relation of the wave which includes the effect of current. The Doppler effect takes it to the boundary condition of the free water surface. Finally, the three-dimensional boundary element is applied to obtain the velocity potential in a wave–current field which is affected by the structures.

According to our method, the interactions among currents, waves and structures can be properly expressed even for the case where the direction between the wave and the current is perpendicular.

REFERENCES

1. Longuet-Higgins, M. S. & Stewart, R. W. The changes in amplitude of short gravity waves on steady non-uniform currents. *Journal of Fluid Mechanics*, 1961, **10**, 529–549.
2. Newman, J. N. The theory of ship motion. *Advances in Applied Mechanics*, 1978, **18**, 221–282.
3. Grue, J. & Palm, E. Wave radiation and wave diffraction from a submerged cylinder in a uniform current. *Journal of Fluid Mechanics*, 1985, **2521**, 257–278.
4. Matsui, T. S. Lee, S. Y. & Sano, K., Hydrodynamic forces on a vertical cylinder in current and waves. *Journal of the Society of Naval Architects of Japan*, 1991, **270**, 277–287 (in Japanese).
5. Chou, C. R. & Han, W. Y. Wave-induced oscillations in harbours with dissipating quays. *Costal Engineering in Japan*, 1993, **36**(1), 1–23